We are IntechOpen,
the world's leading publisher of
Open Access books
Built by scientists, for scientists

6,900
Open access books available

185,000
International authors and editors

200M
Downloads

154
Countries delivered to

Our authors are among the

TOP 1%
most cited scientists

12.2%
Contributors from top 500 universities

BOOK CITATION INDEX
CLARIVATE ANALYTICS
INDEXED

WEB OF SCIENCE™

Selection of our books indexed in the Book Citation Index
in Web of Science™ Core Collection (BKCI)

Interested in publishing with us?
Contact book.department@intechopen.com

Numbers displayed above are based on latest data collected.
For more information visit www.intechopen.com

Tissue Characterization of Carotid Plaques

Masanori Kawasaki, Shinichi Yoshimura and
Kiyofumi Yamada

Additional information is available at the end of the chapter

1. Introduction

Carotid plaque vulnerability has been reported to be associated with stroke and other cerebrovascular events [1, 2]. Therefore, tissue characterization of carotid plaques is important to evaluate the risk of cerebrovascular disease and outcome of treatment for carotid arterial stenosis. Stabilization of vulnerable plaques rather than regression of plaque volume is considered the major contributor to beneficial effects on cerebrovascular events [3].

With respect to the ultrasound technique, ultrasonic tissue characterization of the myocardium with an integrated backscatter (IBS) analysis was developed, which is capable of providing both conventional two-dimensional echographic (2DE) images and IBS images. In studies of the myocardium, calibrated myocardial IBS was significantly correlated with the volume fraction of interstitial fibrosis [4, 5]. In preliminary *in vitro* studies, IBS values reflected the structural and biochemical composition of atherosclerotic lesion and could differentiate fibrofatty, fatty and calcification of arterial walls [6-8]. However, it is not precise, because IBS values of lipid pool and intimal hyperplasia were similar. Discrimination of intimal hyperplasia, fibrous cap and thrombus, and sensitivity and specificity of these measurements were not studied in these papers. Furthermore, extent evaluation of each composition, that is, two-dimensional (2D) tissue structure, in entire plaque has not been examined. Therefore, we measured IBS values in carotid arteries in patients compared before and immediately after death, and compared these IBS values with their histopathological features. Subsequently, we constructed 2D color-coded maps of arteries with plaque to assess visually the arterial tissue characteristics.

2. Comparison between IB values and histological images in carotid arteries

Conventional echo images and IBS images were acquired using an ultrasonic imaging system (Sonos 5500, Philips Medical Systems) to characterize the carotid arterial tissue at the bedside conveniently using a 5-12 MHz multifrequency transducer for all studies. This software enabled the acquisition, storing and retrieving of a sequence of continuous 2D conventional and IB images, forming a continuous loop digital recording of two seconds (60 frames in two seconds). Off-line analysis of the 2D IBS images was performed by retrieving the previously stored data from the built-in optical disc drive in the system. IBS value was calculated as the average power of the ultrasound backscattered signal from a small volume of tissue measured in decibels (dB). We used an 11 x 11 pixels (0.6 mm x 0.6 mm) rectangle shaped ROI and set the time gain compensation at 0 dB and the lateral gain compensation at 50 dB at every measurement in both *ex vivo* and *in vivo* study. At this setting, IBS values of stainless steel at a distance of one to two centimeters from the transducer were 50 dB, which was within the dynamic range of the system. IBS values of the posterior arterial wall were corrected (corrected IBS) by subtracting the IBS values of the vessel lumen.

Carotid arteries were excised at autopsy and were fixed with 10% neutral buffered formalin. Ring-like arterial specimens obtained at a similar level to the ultrasound study were decalcified in a standard K-CX solution for five hours, and were embedded with paraffin and cut into 4 μm thick transverse sections perpendicular to the longitudinal axis of the artery. They were stained with hematoxylin-eosin, elastic van Gieson and Masson's trichrome. In addition, immunohistochemical analysis using anti-actin antibody was performed for detection of smooth muscle cells.

Histology of these sampling sites was divided into thrombus (n=5), lipid pool (n=31), intimal hyperplasia (n=7), fibrosis (n=25), mixed lesion (n=12) and calcification (n=17) in the intima, and the media (n=24). Each corrected IBS value of these tissues after fixation at autopsy was 7.3 ± 1.5, 13.0 ± 3.2, 10.9±1.0, 19.3 ± 2.4, 28.2 ± 3.3 and 39.3 ± 3.6 in the intima, respectively, and 11.3 ± 1.9 dB in the media. Also each corrected IBS value during lifetime was 4.9 ± 1.0, 10.0 ± 2.4, 8.0±0.8, 16.0 ± 2.0, 23.5 ± 3.4 and 30.5 ± 2.5 in the intima, respectively, and 8.4 ± 1.8 dB in the media. The difference among thrombus, fibrosis (category-3), mixed lesion, calcification and lipid pool, intimal hyperplasia or media were statistically significant. However, lipid pool, intimal hyperplasia and media had similar IBS values (category-2) [9]. In category-2, the media and intima were differentiated using conventional 2DE. Generally, the lipid pool (category-2) is anatomically located under a fibrous cap consisting of fibrosis (category-3). Therefore, the presence of ROIs with category-2 under a layer of ROIs with category-3 was defined as the lipid pool, but not as intimal hyperplasia.

Based on the above definitions using *in vivo* 2DE and IBS color-coded maps of tissue characterizations were constructed in *in vivo* images. These also reflected the pathology well (Figure 1).
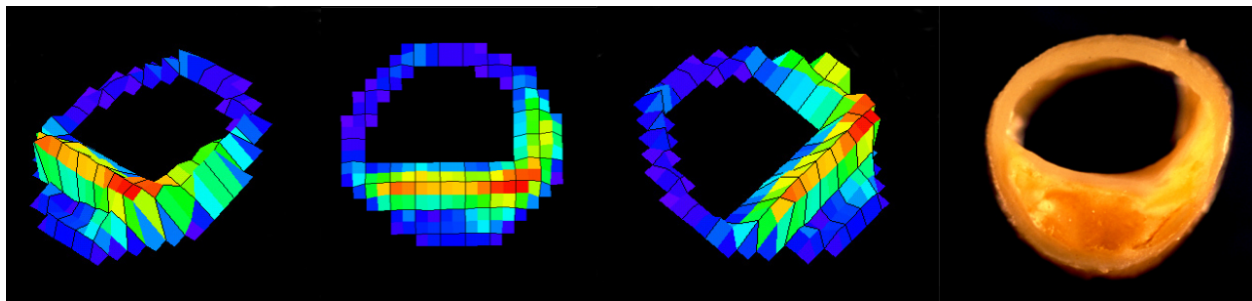
Figure 1. Integrated backscatter ultrasound color-coded maps of the carotid plaque. Left: color-coded maps (red: calcification, orange: mixed lesion, green: fibrosis, blue: lipid pool). Right: pathological specimen.

3. Effects of statin on carotid atherosclerotic plaques

Several large clinical trials have demonstrated that lipid-lowering therapy with HMG-Co-A reductase inhibitors, (statins), reduces cerebrovascular events [10, 11]. Stabilization of vulnerable plaques rather than regression of plaque volume is considered the major contributor to this beneficial effect (5). Stabilization of vulnerable plaques rather than regression of plaque volume is considered the major contributor to this beneficial effect [3].

We assessed the effect of a strong lipophilic statin (atorvastatin) on the stabilization of carotid plaques with ultrasound IBS color imaging by calculating the relative lipid volume. We enrolled patients who were diagnosed with asymptomatic carotid artery stenosis (30-60%) based on carotid ultrasonography and MR angiography. The patients were randomized to a statin (atorvastatin 20mg/day) treatment group (n = 20) or a diet group (n = 20). Transverse and longitudinal scans of carotid plaques were performed using an ultrasound imaging system (SONOS 7500, Philips Medical Systems). The plaques which have unstable component such as lipid core or necrotic core were also imaged with a 1.5-T magnetic resonance imaging (MRI) system (Intera Achieva Nova Dual, Philips Medical Systems) equipped with standard neck array coils. T1-weighted (T1W), proton density-weighted (PDW), and T2-weighted (T2W) images as well as time-of-flight (TOF) images of the plaques were obtained by standardized protocol. The components of plaque were assessed using previous established criteria [12]. We calculated the ratio of the signal intensity of carotid plaques to that of sternocleidomastoid muscle and defined this as the signal intensity ratio (SIR).

At baseline, clinical parameters did not differ between groups. After initiating statin therapy, the lipid profile significantly improved in the statin group, but remained unchanged in the diet group. Baseline IBS values and other characteristics and parameters were similar between the study groups. At baseline, no significant differences were found in these parameters between the statin and diet groups. The relative lipid volume significantly increased in the statin group after 6 months (Figure 2). However, IBS values did not change significantly in the diet group.
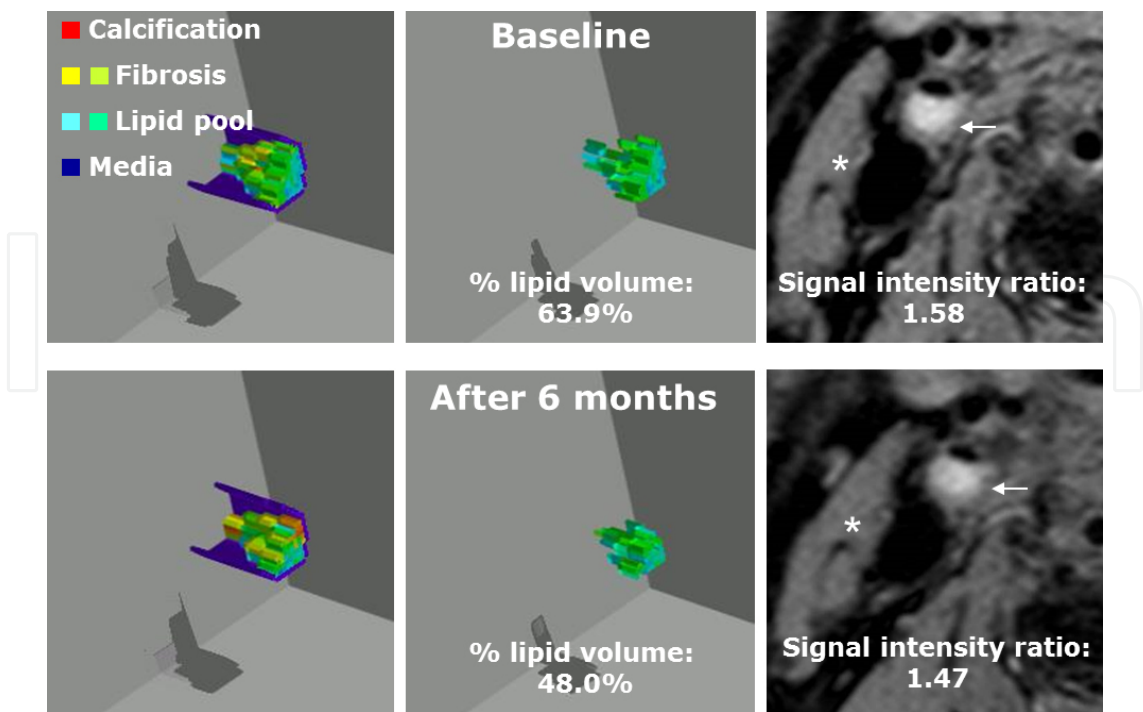
Figure 2. Representative images of three dimensional IBS color-coded maps. Left: Three-dimensional cut out images of color-coded maps of carotid arteries. Middle: Three-dimensional images of lipid pool. Right: High resolutional magnetic resonance images of carotid plaques.

4. Prediction of silent ischemic lesions after carotid artery stenting using IBS and MRI

Carotid artery stenting (CAS) has recently emerged as a potential alternative to carotid endarterectomy (CEA) [13] because it is a less invasive procedure and results in a shorter duration of hospitalization. Although many advantages of CAS have been reported, one of its disadvantages is the considerably high incidence of distal emboli during CAS, even though they are subclinical. Asymptomatic or silent ischemic lesions were detected by diffusion-weighted magnetic resonance imaging (DWI) more often in CAS than in CEA patients [14]. We and other investigators reported that analysis of carotid plaques using IBS ultrasound or black-blood magnetic resonance imaging (BB-MRI) can identify the histological components of carotid plaques [9, 12, 15].

We evaluated carotid lesion with stenosis with a symptomatic carotid stenosis of > 70% or an asymptomatic carotid stenosis of > 60% assessed with angiography, as recommended by the North American Symptomatic Carotid Endarterectomy Trial collaborators [16]. In IBS analysis, relative unstable component area (%UCA: area of intra-plaque hemorrhage and lipid pool / area of plaque) were automatically measured in each plaque by computer software (T3D, Fortner Research LLC, Sterling, Virginia). IN MRI analysis, we calculated the ratio of the signal intensity of carotid plaques to that of sternocleidomastoid muscle and defined this as the signal

intensity ratio (SIR). We assessed newly appearing ipsilateral silent ischemic lesions (NISIL) detected by diffusion-weighted magnetic resonance imaging (DWI) before and after CAS. At the same time, we performed quantitative analysis of plaque characteristics using IBS ultrasound and BB-MRI before CAS in all patients.

After CAS, DWI showed 94 silent ischemic lesions in 19 patients (38%) (diffusion positive group; P group). There were no differences in baseline patient characteristics between the P group and diffusion negative group (N group). In the P group, %UCA analyzed by IBS was significantly higher than in the N group ($60.2 \pm 23.4\%$ and $35.3 \pm 19.2\%$, respectively, p<0.001). Also, the SIR of most stenotic lesions of carotid plaques analyzed by T1WI of BB-MRI was significantly higher in the P group than in the N group (1.40 ± 0.19 and 1.18 ± 0.25, respectively, p<0.01) (Figure 3). In multivariate logistic regression analysis, the independent predictors of NISIL were SIR (p = 0.030), the CRP level (p = 0.041) and the %UCA measured by IBS (p = 0.049). In the analysis of receiver operating characteristic curves, 50% of the %UCA measured by IBS analysis and an SIR of 1.25 measured by BB-MRI analysis were determined as the most reliable cutoff values for predicting NISIL. Using these cutoff values, the respective positive and negative predictive values were 76% and 82% in the IBS analysis and 62% and 88% in the BB-MRI analysis.
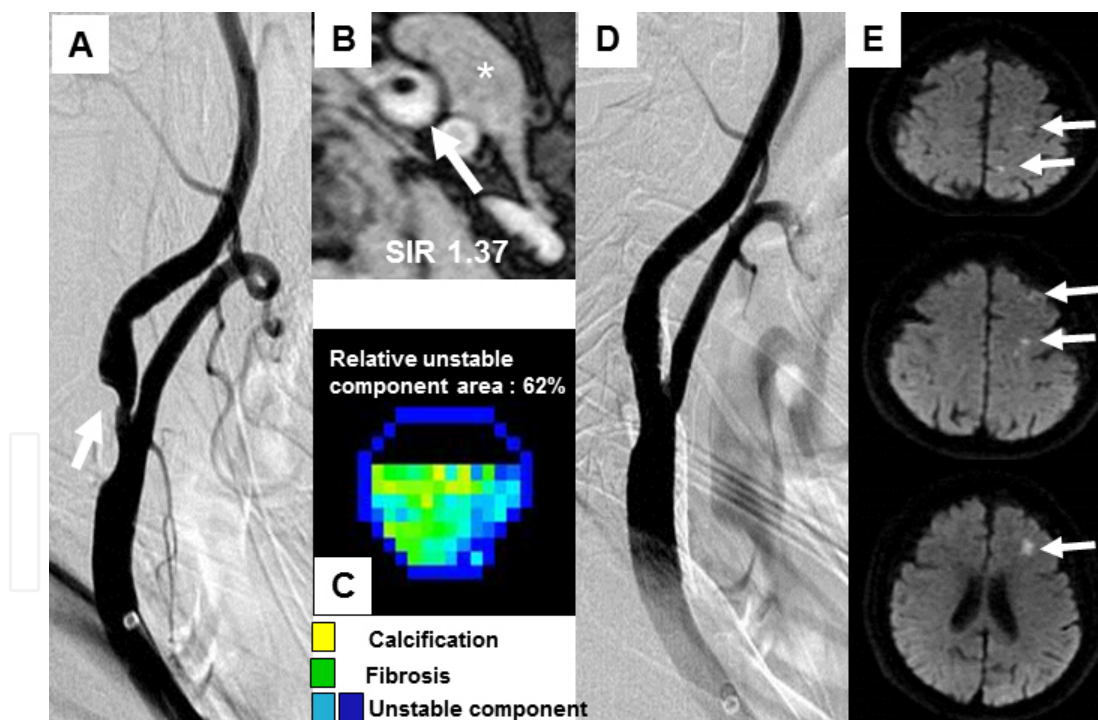

Figure 3. Representative images of CAS for an internal carotid plaque that consisted of less unstable component. (A) Pre-steting angiogram of the left internal carotid artery stenosis. (B) White arrow: Axial image of the most stenotic lesion of the plaque on T1WI of BB-MRI. *: sternocleidomastoid muscle. The SIR was 1.37 (C) Cross-sectional color-coded map of the most stenotic lesion of the plaque on IBS. Relative unstable component area was 62%. (D) Post-stenting angiogram of the left internal carotid artery stenosis. After carotid artery stenting, the lumen of the right internal carotid artery was successfully dilated. (E) Diffusion-weighted magnetic resonance imaging. White arrows: multiple silent ischemic lesions are detected in the left cerebral hemisphere after the post-stenting procedure.

5. Plaque feature of the internal carotid plaques evaluated by optical coherence tomography

Recently, intravascular optical coherence tomography (OCT) provides high-resolution, cross-sectional images of tissue in situ and has an axial resolution of 10 μm and a lateral resolution of 20 μm [17, 18]. The OCT images of human coronary atherosclerotic plaques obtained in vivo provide additional, more detailed structural information than intravascular ultrasound [19].

By applying this technique to carotid plaques, we previously reported the first case of cerebral infarction due to plaque rupture that could be visualized by OCT in the internal carotid artery [20]. An 83-year old male was admitted to our hospital due to newly developed motor weakness of the left hand. MRI-DWI showed multiple high intensity spots in the territory of the middle cerebral artery, and an initial MRA revealed significant stenosis at the origin of the right internal carotid artery. After angiography, a 9-F guiding catheter with an occlusion balloon was navigated to the right common carotid artery and a guidewire with an occlusion balloon (Guardwire, Medtronic Japan Co., Ltd., Tokyo, Japan) was introduced into the external carotid artery. Carotid angiography revealed apparent changes of the wall morphology of the stenotic site, suggesting an enlargement of intraluminal thrombus (Figure 4), which is considered a risk
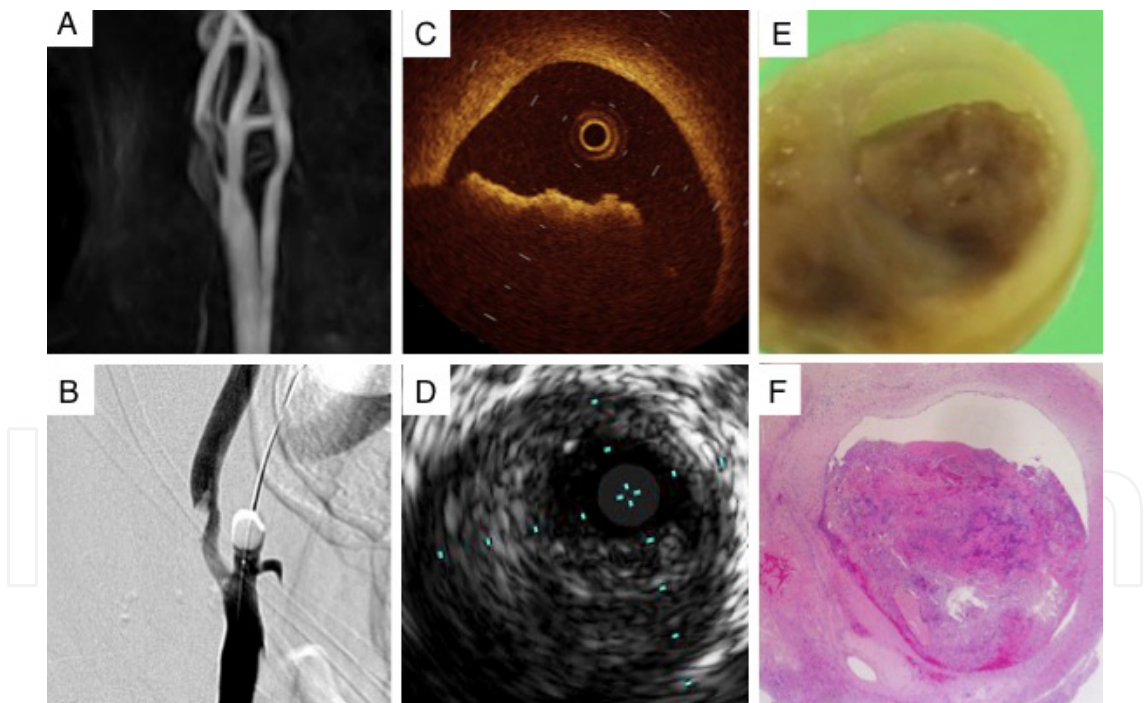

Figure 4. Optical coherence tomography of the internal carotid artery and pathological findings. A: An initial magnetic resonance angiography revealed severe stenosis of the internal carotid artery and high intensity plaque. B: The carotid angiogram showed internal carotid artery stenosis and enlargement of an intraluminal protrusion in the internal carotid artery. C: Cross-sections by the optical coherence tomography (OCT) demonstrated intraluminal thrombus with shadowing in the internal carotid artery. D: Cross-sections by intravascular ultrasound showed only eccentric and low-echoic plaque in the internal carotid artery. E: Macroscopic view of surgical specimen revealed intraluminal thrombus formed at the ruptured site of the soft plaque. F: Pathological analysis with Hematoxylin-Eosin staining confirmed soft plaque and intraluminal red thrombus which coincided with OCT findings.

factor for stenting. To confirm the presence of intraluminal thrombus, the stenotic site was imaged with OCT (Image Wire, Light-lab imaging, Goodman, Co, Ltd, Nagoya, Japan) using an automatic pull-back device from the distal portion at 1 mm/s. OCT clearly revealed an intraluminal thrombus (Figure 4-C), and a tear of a fibrous cap with ulceration at the more proximal internal carotid artery. Carotid artery stenting was cancelled due to enlarged thrombus being considered a high risk factor, and carotid endarterectomy was performed the next day. The specimen obtained during endarterectomy showed soft plaque and intraluminal thrombus which coincided with OCT findings performed preoperatively (Figure 4-E, F).

6. Assessment of arterial medial characteristics in carotid arteries using integrated backscatter ultrasound

In general, atherosclerotic changes consist of two components: atherosis and sclerosis. According to a pathological study, these changes are recognized as thickening of intima-media thickness (IMT) which is associated with structural atheromatous changes and decreased
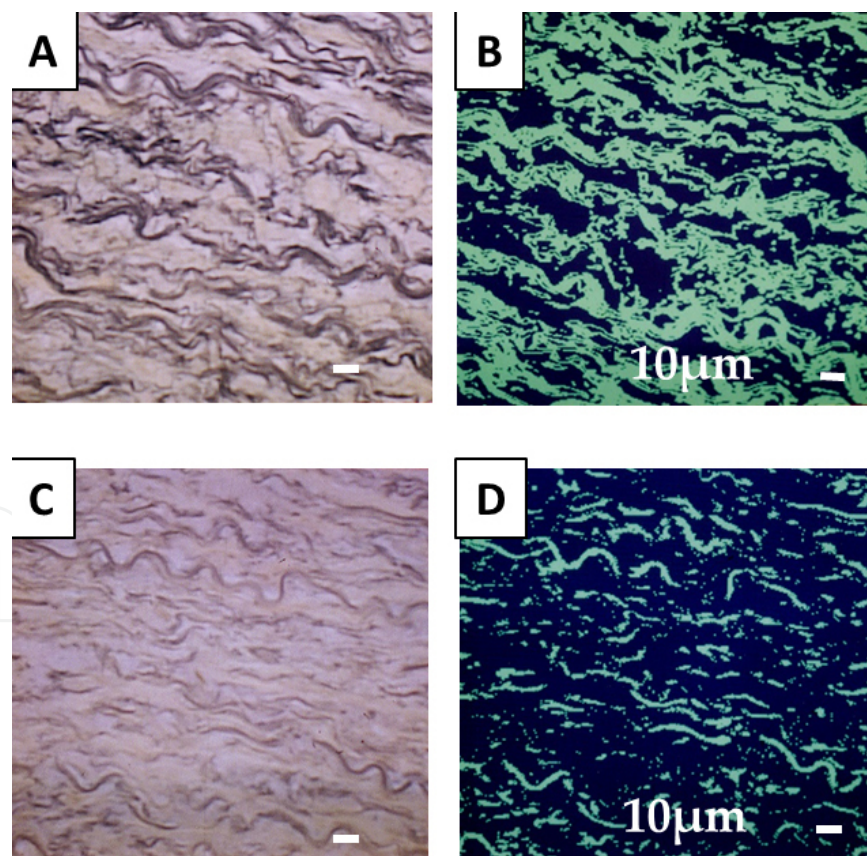

Figure 5. Representative histological images of carotid media. (A) (C) Histological images stained by elastic van Gieson staining. (B) (D) Digitized images, in which elastic fibers were selected by the following thresholding of the digital image LUZEX F (Nireco, Kyoto, Japan). (B) Elastic fiber index: 59.3 %, Elastic fragmentation index: 57.7 % and IBS value: 9.1 dB. (D) Elastic fiber index: 18.9 %, Elastic fragmentation index: 79.3 % and IBS value: 14.4 dB.

extensibility which is associated with functional sclerotic changes in elastic and collagen fibers. There are several ultrasound parameters to evaluate atherosclerosis, such as IMT, which is associated with atheromatous plaque formations and stiffness ß, which are associated with decreased extensibility of the arterial wall. IMT measurement is widely performed for the detection of atheromatous lesions and associated with age and coronary risk factors [21, 22]. However, IMT is not always associated with the severity of arterial sclerosis in patients with hypertension [23]. This may be due to the degenerative changes in the medial smooth muscle cells and variably increased amount of elastin and collagen in hypertensive vessels [24].

The elasticity of major arteries is also affected by cardiovascular risk factors such as hypertension, hyperlipidemia, diabetes and aging. Stiffness ß, which was defined by Hayashi et al was found to be independent of blood pressure in the physiological range and associated with the severity of coronary atherosclerosis [25-27]. An increase in arterial stiffness has been reported as an early sign of atherosclerosis [28]. Therefore, it is very important to evaluate arterial sclerosis non-invasively. We showed that IBS values of carotid media were correlated with the stiffness of carotid arteries, and those were also correlated with elastic fiber fragmentation index (Figure 5) [29].

7. Conclusion

Recently, many techniques for the tissue characterization of human carotid arteries have been established. IBS, MRI and OCT are promising techniques to assess the degree of atherosclerotic lesions in carotid artery and predict cerebrovascular disease.

Author details

Masanori Kawasaki[1*], Shinichi Yoshimura[2] and Kiyofumi Yamada[2]

*Address all correspondence to: masanori@ya2.so-net.ne.jp

1 Department of Cardiology, Gifu University Graduate School of Medicine, Gifu, Japan

2 Department of Neurosurgery, Gifu University Graduate School of Medicine, Gifu, Japan

References

[1] Polak JF, Shemanski L, O'Leary DH, Lefkowitz D, Price TR, Savage PJ, Brant WE, Reid C. Hypoechoic plaque at US of the carotid artery: An independent risk factor for incident stroke in adults aged 65 years or older. The Cardiovascular Health Study. Radiology 1998;208:649–654.

[2] Gronholdt ML, Nordestgaard BG, Schroeder TV, Vorstrup S, Sillesen H. Ultrasonic echolucent carotid plaques predict future strokes. Circulation 2001;104:68-73.

[3] Libby P, Aikawa M. Stabilization of atherosclerotic plaques new mechanisms and clinical targets. Nat Med 2002;8:1257-1262.

[4] Picano E, Pelosi G, Marzilli M, Lattanzi F, Benassi A, Landini L, L'Abbate A. In vivo quantitative ultrasonic evaluation of myocardial fibrosis in humans. Circulation. 1990; 81:58-64.

[5] Naito J, Masuyama T, Mano T, Kondo H, Yamamoto K, Nagano R, Doi Y, Hori M. Ultrasound myocardial tissue characterization in the patients with dilated cardiomy-opathy: Value in noninvasive assessment of myocardial fibrosis. Am Heart J. 1996;131:115-121.

[6] Barziliai B, Shffitz JE, Miller JG, Sobel BE. Quantitative ultrasonic characterization of the nature of atherosclerotic plaques in human aorta. Circ Res.1987; 60: 459-463.

[7] Urbani MP, Picano E, Parenti G, Mazzarisi A, Fiori L, Paterni M, Pelosi G, Landini L. In vivo radiofrequency-based ultrasonic tissue characterization of the atherosclerotic plaque. Stroke. 1993;24:1507-1512.

[8] Picano E, Landini L, Lattanzi F, Salvadori M, Benassi A, L'Abbate A. Time domain echo pattern evaluation from normal and atherosclerotic arterial walls: a study in vi-tro. Circulation. 1988;77:654-659.

[9] Kawasaki M, Takatsu H, Noda T, Ito Y, Kunishima A, Arai M, Nishigaki K, Take-mura G, Morita N, Minatoguchi S, Fujiwara H. Non-invasive tissue characterization of human atherosclerotic lesions in carotid and femoral arteries by ultrasound inte-grated backscatter. -Comparison between histology and integrated backscatter im-ages before and after death- J Am Coll Cardiol. 2001;38:486-492

[10] Amarenco P, Bogousslavsky J, Callahan A 3rd, Goldstein LB, Hennerici M, Rudolph AE, Sillesen H, Simunovic L, Szarek M, Welch KM, Zivin JA; Stroke Prevention by Aggressive Reduction in Cholesterol Levels (SPARCL) Investigators. High-dose ator-vastatin after stroke or transient ischemic attack. N Engl J Med 2006;355:549-559.

[11] Waters DD, Schwartz GG, Olsson AG, Zeiher A, Oliver MF, Ganz P, Ezekowitz M. For the MIRACLE study investigator. Effects of atorvastatin on stroke in patients with unstable angina or non-Q-wave myocardial infarction. A Myocardial ischemia reduction with aggressive cholesterol lowing (MIRACLE) substudy. Circulation 2002;196:1690-1695.

[12] Yuan C, Mitsumori LM, Ferguson MS, Polissar NL, Echelard D, Ortiz G, Small R, Da-vis JW, Kerwin WS, Hatsukami In vivo accuracy of multispectral magnetic resonance imaging for identifying lipid-rich necrotic cores and intraplaque hemorrhage in ad-vanced human carotid plaques. Circulation 2001;104:2051-2056.

[13] Diethrich EB, Ndiaye M, Reid DB. Stenting in the carotid artery: initial experience in 110 patients. J Endovasc Surg. 1996;3:42-62.

[14] Schnaudigel S, Gröschel K, Pilgram SM, Kastrup A. New brain lesions after carotid stenting versus carotid endarterectomy: A systematic review of the literature. Stroke 2008;39:1911-1919.

[15] Kawasaki M, Ito Y, Yokoyama H, Arai M, Takemura G, Hara A, Ichiki Y, Takatsu H, Minatoguchi S, Fujiwara H. Assessment of arterial medial characteristics in human carotid arteries using integrated backscatter ultrasound and its histological implications. Atherosclerosis 2005;180:145-54.

[16] North American Symptomatic Carotid Endarterectomy Trial Collaborators: Beneficial effect of carotid endarterectomy in symptomatic patients with high-grade carotid stenosis. N Engl J Med 1991;325:445-453.

[17] Tearney GJ, Brezinski ME, Bouma BE, Boppart SA, Pitris C, Southern JF, Fujimoto JG. In vivo endoscopic optical biopsy with optical coherence tomography. Science. 1997; 276:2037–2039.

[18] Brezinski ME, Tearney GJ, Bouma BE, Izatt JA, Hee MR, Swanson EA, Southern JF, Fujimoto JG. Optical coherence tomography for optical biopsy: properties and demonstration of vascular pathology. Circulation. 1996; 93:1206–1213.

[19] Jang IK, Tearney GJ, MacNeill B, Takano M, Moselewski F, Iftima N, Shishkov M, Houser S, Aretz HT, Halpern EF, Bouma BE. In vivo characterization of coronary atherosclerotic plaque by use of optical coherence tomography. Circulation. 2005;111:1551-1555.

[20] Yoshimura S, Kawasaki M, Yamada K, Enomoto Y, Hattori A, Nishigaki K, Minatoguchi S, Iwama T. Determination of intraluminal thrombus in the carotid artery by optical coherence tomography: a case report. Neurosurgery 2010;67:onsE305.

[21] Hadjiisky P, Peyri N, Grosgogeat Y et al. Tunica media changes in the spontaneously hypertensive rat (SHR). Atherosclerosis. 1987;65:125-137.

[22] Mannami T, konishi M, baba S et al. Prevalence of asymptomatic carotid atherosclerotic lesions detected by high-resolution ultrasonography and its relation to cerdiovascular risk factors in the general population of a Japanese city. Stroke. 1997;28:518-525.

[23] Rossi M, Cupisti A, Perrone L et al. Carotid ultrasound backscatter analysis in hypertensive and in healthy subjects. Ultrasound Med Biol. 2002;28(9):1123-1128.

[24] Wolinsky H. Response of the rat aortic media to hypertension. Circ Res. 1970;26:507-522.

[25] Ebrahim S, Papacosta O, Whincup P et al. Carotid plaque, intima media thickness, cardiovascular risk factors, and prevalent cardiovascular disease in men and women. The British regional heart study. Stroke. 1999;30:841-850.

[26] Hirai T, Sasayama S, Kawasaki T et al. Stiffness of systemic arteries in patients with myocadial infarction. A noninvasive method to predict severity of coronary athero-sclerosis. Circulation. 1989;80:78-86.

[27] Hayashi K, Handa H, Nagasaka S et al. Stiffness and elastic behavior of human intra-cranial and exracranial arteries. J Biomech. 1980; 13: 175-184

[28] Ferrier KE, Muhlmann MH, Baguet JP et al. Intensive cholesterol reduction lowers blood pressure and large artery stiffness in isolated systolic hypertension. J Am Coll Cardiol. 2002; 39: 1020-1025.

[29] Kawasaki M, Ito Y, Yokoyama H, Arai M, Takemura G, Hara A, Ichiki Y, Takatsu H, Minatoguchi S, Fujiwara H. Assessment of arterial medial characteristics in human carotid arteries using integrated backscatter ultrasound and its histological implica-tions. Atherosclerosis. 2005;180:145-54.